# Advances in Neural Network assisted Tool Pressure Prediction

*Florian* Göltl[1*], *Felix* Harst[2], *Arndt* Birkert[1] and *Nicolaj C.* Stache[2]

[1]Center for Metal Forming and Car Body Manufacturing, Faculty of Mechanics and Electronics, Heilbronn University of Applied Sciences, 74081 Heilbronn, Germany
[2]Center for Machine Learning, Faculty of Mechanics and Electronics, Heilbronn University of Applied Sciences, 74081 Heilbronn, Germany

**Abstract.** In car body tool engineering spotting patterns are used to validate the quality of the tool active surfaces. The objective is to display a homogeneous pressure distribution at defined drawing depths, as achieved by setting the parameters in the simulation accordingly. However, the qualitative evaluation of pressure distribution performed by human visual inspection of spotting patterns is not sufficient for quantitative analysis. It has been demonstrated that convolutional neural networks (CNNs) can predict pressure distributions from spotting patterns. This publication examines the impact of color quantity and contact pairing on the formation of spotting patterns. Likewise, the repeatability of spotting images is evaluated at the macro-, meso- and microscopic levels. A CNN based regression model estimates the absolute pressure distribution based on images of spotting patterns. The integral force, calculated from the estimated pressure distribution, is compared with the measured process force and used either for validation or as part of the CNN output post-processing. In this process, the CNN output is scaled to absolute values using the known total integral force, allowing the post-processing method to extrapolate the predicted pressure distribution effectively, even in untrained regions.

**Keywords:** Machine Learning; CNN; Tool Tryout; Experimental Data

## 1 Introduction

Car body production is moving towards full automation, increasingly integrating virtual twins and digital shadows in sheet metal forming. This shift is driven by advancements in finite element (FE) modeling and the growing availability of measurement data for machines, tools, and workpieces. Data-driven models and algorithms can be implemented to enhance the traditional engineering of car body tools and/or to objectify empirical procedures like car body tool processing. Currently, the total cost of tryout accounts for 25-35% of tooling costs and presents a significant opportunity for cost reduction [1].

Despite the considerable investment in the development of car body tools and the associated forming processes, as well as the implementation of virtual analyses using finite element (FE) simulations, the manual, experience-based tool tryout remains indispensable. This leads to extended press utilization times and limited efficiency. The evaluation of pressure is a critical aspect of tool processing, where the quality of the tool's interaction with the workpiece is determined by the spotting patterns generated during the forming process. The sheet metal part and forming tool are closed and reopened in the car body press. A spotting paste between the workpiece and the tool indicates contact points and pressure distributions. The high-pressure areas displace the spotting paste, while the untouched areas leave it unchanged. A visual inspection of the pressure distribution shows workers where to remove material. Local changes in load-bearing behavior can shift the global behavior, requiring iterative adjustments by experts. Differences between simulated and actual pressure images are attributed to manufacturing inaccuracies, changing sheet thickness during forming and the press-tool-system's elastic behavior. The discrepancies of the latter are empirically mitigated through counter-bending of the active tool surfaces. However, achieving sub-millimeter precision, contingent on the deflection compensation method, necessitates tool processing during tryout.

The relevant spotting patterns are typically determined shortly after the initial blankholder contact and again at or just before bottom dead center (BDC). The precise values for the evaluation vary depending on the specific tooling shop and the original equipment manufacturer (OEM). For example, *blank holder closure* is typically analyzed a few millimeters after the initial blank holder contact, where a homogeneous contact pattern with an 80% contact ratio is employed as a quality criterion. In practice, there is an absence of uniform specifications for the application of the spotting paste. The paste is applied with brushes or paint rollers, and the amount of paste is determined at the discretion of the skilled worker. This approach can result in inconsistencies in the quantity of paint applied to an inked sheet, which, in turn, can have a subtle effect on the properties of the resulting spotting pattern. The application of spotting paste in specific areas may be reduced, causing these areas to appear lighter upon visual inspection, and giving the impression of a higher pressure. Subsequent differentiation is not possible, even for experts. A series of expert interviews with regional German tool shops has indicated an increasing relocation of tool processing to low-wage countries.

* florian.goeltl@hs-heilbronn.de

This has resulted in the majority of work being carried out abroad, with final rework and adjustments being conducted in the established tool shops. Obtaining the support of experienced European tool mechanics can be both time-consuming and costly.

The significance of quantifiable pressure distribution has been highlighted by the scientific research conducted in recent years. Essig's research has demonstrated the efficacy of incorporating image data from spotting patterns into FE models. This approach has been shown to enhance the prediction accuracy by adapting the models to the actual bearing areas, even under the assumption of an ideally rigid press and die [2, 3]. Zabala et al. have investigated the correlation between paste distribution and pressure values for small, simple rectangular dies and proposed an algorithm for the relative evaluation of spotting patterns [4].

In our previous research, we demonstrated the capacity of CNNs to estimate pressure values based on a spotting pattern. The investigation focused on one contact pairing within the examined pressure range of 0.5 to 3 MPa. To this end, the pressure values were measured on the flat contact surfaces using a PreScale pressure-sensitive film from Fuji, and the corresponding spotting images were photographed with a constant amount of color. This process yielded 37,450 data points, of which 50% were used for training and the remaining 50% for validation and testing. The predictions of the CNN were found to be acceptable, though they exhibited discernible deviations [5].

In the absence of a substantial volume of measurement data concerning pressure distributions, it is rational to rely on synthetic data, such as that derived from FE simulations. Hohmann et al. presents a data-driven artificial intelligence (AI) method to enhance the tool try-out process in deep drawing. The authors propose an encoder-decoder model trained on simulated pressure distributions to predict the active tool surface, addressing the complex interactions between tools, sheet metal, and press. The efficacy of the proposed method is substantiated through a comparative analysis with state-of-the-art approaches, namely U-Net and Pix2Pix [6].

It is crucial to acknowledge the limitations of synthetic data, which are contingent on the model from which they are derived. Consequently, their accuracy is inherently constrained and may not fully align with reality. Measurement data is susceptible to random errors though.

In contrast to the findings of previous studies, the present work focuses on the influence of ink quantity, material, surface texture and its dependence on the blank preload condition on the spotting pattern. In addition to this impact on CNN-based pressure prediction, this analysis also includes the dependency of these spotting patterns over an extended pressure range.

## 2 Methods and procedures

The objective of this publication is to present a methodology that enhances the objectivity and efficiency of the spotting process. This approach mitigates the time and personnel uncertainties that are inherent in manual processes. To improve the proposed CNN's prediction quality of the pressure distribution large data is required.

### 2.1 Dataset Generation – generating and measuring spotting patterns

The quality of the incoming data is imperative for a machine learning approach to describing physical systems. To ensure the repeatability of the spotting images, the spotting paste is applied to the sheet using a plastic roller and is distributed evenly. The average amount of paint in g/m² can be determined by measuring the weight of the paint roller and the spotting paste before and after application and calculating the difference. This method has proven effective not only with smaller test tools but also with larger blanks of car body tools. Two pressure disks, each with a diameter of 90 mm, are employed as tools for generating spotting patterns (see Fig.1). Precise alignment of the two tool surfaces, correlating to a processed tool, is ensured by two fitting holes positioned on different bolt circle diameters. All tests were performed on a Zwick/Roell Z100 tensile testing machine, and the force-displacement curves were recorded. The measurement concluded upon reaching the targeted pressure, with the contact area pre-entered the system.

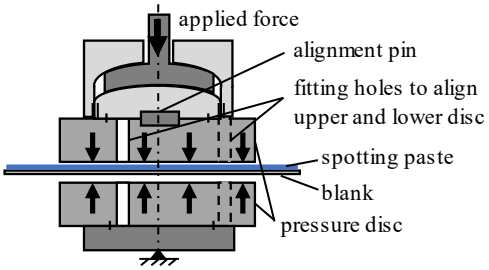


**Fig. 1.** Schematic representation of the measurement method for generating spotting patterns

For analysis, the surface pressure between the tool and the workpiece is examined using spotting paste and a pressure-sensitive film. The latter can provide a quantitative, discrete distribution of values. The film is only suitable for specific measuring ranges, so multiple layers must be used to measure pressures from 0.5 to 8 MPa. With a total thickness of 0.18 mm, the film consists of two components. One side contains a micrometer-range coated reagent that ruptures under specified pressure, allowing the stored chemical to react with the developer film. The resulting color distribution and intensity correlates with the applied contact force. The films are then separated and evaluated for pressure values. However, Fuji's PreScale film is not recommended for double-curved surfaces due to crumpling issues, leading to unreliable results. The film's precision is ±10% of the measured value. Spotting images and pressure measurements are always taken in pairs, with tool contact surfaces cleaned after each image.

The Canon EOS R SLR camera (24.2 MP) with a Canon EF 100mm macro lens was utilized to capture the spotting images on a macroscopic scale. The circular

spotting patterns have dimensions of 2000 pixels by 2000 pixels (px), which corresponds to a resolution of 22 px/mm. The images were captured against a uniform gray background to perform white balancing. Microscopic measurements were conducted utilizing a 3D laser scanning microscope (VK-X3000, Keyence). Magnification levels of 5 times are considered mesoscopic, while those of 10 times and above are microscopic.

## 2.2 Variables of spotting patterns

The examination focuses on how the material, surface topology, ink quantity, and preloading status influence the spotting patterns concerning the applied pressure. The temperature and humidity levels remained constant within the established parameters, fluctuating within the range of 21-23°C and 45-49%, respectively. To ensure the reliability of the findings, the respective measurements were repeated on two separate occasions. This approach was adopted to both validate the results and augment the test data.

**Table 1.** Measured spotting patterns with a dependency combination of material, surface topology, ink quantity, preload status and pressure for two anisotropic uniformly textured blanks (precision textured, electrical discharge texturing) and one isotropic surface (mill finished).

| material | steel | aluminum | aluminum |
|---|---|---|---|
| surface topology | PreTex | EDT | MF |
| blank thickness | 1.0 mm | 1.0 mm | 1.0 mm |
| Sa/Sz for $A_{ref}$ = 4mm² | 1.5/22.2 µm | 1.5/27.7 µm | 1.2/22.7 µm |
| ink quantity in g/m² | 7.5-8.34 | 5.5-6.5<br>7.5-8.34<br>9.5-10.5 | 7.5-8.34 |
| preloading status | y/n | y/n | y/n |
| pressure loads in MPa | 1, 2, 3, 4, 7<br>(five loads) | 0.5, 1, 1.5, 2, 2.5, 3, 4, 5, 6, 7, 8<br>(eleven loads) | 1, 2, 3, 4, 7<br>(five loads) |
| base + repeat measurements | 1+2 | 1+2 | 1+2 |
| total measurements | 30 | 198 | 30 |

The materials utilized in this study encompass deep-drawing steel DC05 and aluminum EN AW 6016. The galvanized steel sheet is distinguished by a precision textured surface topology (PreTex®, Salzgitter Flachstahl GmbH), while the aluminum sheet offers both a Mill Finish (MF, AMAG) and an Electron Discharge Texturing (EDT, AMAG) surface topology. In alignment with the practical application quantities of spotting paste, three distinct ranges are categorized within the scope of process-related fluctuations. The low ink quantity is 5.5-6.5 g/m², the medium quantity is 7.5-8.34 g/m², and the high quantity is 9.5-10.5 g/m². However, higher values are also employed in practice, though no subjectively perceptible changes in the spotting pattern were observed. A further increase in the amount of ink results in a more pronounced appearance of the edge areas of spotting images, where ink accumulation occurs due to the pressure load.

The influence of preload conditions on spotting pattern characteristics is further analyzed. Spotting patterns are documented at various drawing depths, indicating that the sheet metal undergoes partial forming. This process alters the surface of the sheet, leading to leveling phenomena. A spotting pattern that occurs at or shortly after sheet blank holder closure undergoes negligible to minimal strain, while in BDC, the sheet is fully formed, the component is colored, and it is reinserted into the tool and reloaded. The observed pressures range from 0.5 MPa to 8 MPa and are divided into eleven measurement points. To optimize the complexity of the measurements, certain combinations were examined only to a limited extent. The number of measurements can be seen in detail in table 1.

## 2.3 Preprocessing of data & Machine Learning Model

In a first step the 2D pressure measurements were converted into a continuous distribution by applying a Gaussian smoothing approach. First, a mask was generated to exclude cylindrical and borehole regions from further processing. A Gaussian filter with a standard deviation of σ=15 px (corresponding to approximately 3.5 mm) was then applied to smooth the measured pressure values. To correct for edge artifacts introduced by the filtering process, the values were normalized by dividing by the surface integral of the masked Gaussian filter.

To ensure consistency between the pressure measurement data and the corresponding contact images, both datasets were aligned and cropped to a common reference frame. This step ensured that extracted features from the contact images were accurately mapped to their corresponding pressure values.

For robust model training and evaluation, the dataset was split into training, validation, and test sets. To avoid spatial correlations between adjacent samples, the contact images were divided into non-overlapping segments. This ensured that extracted samples from the same image were sufficiently separated, preventing information leakage between the training and validation/test sets. Each extracted data sample consisted of a corresponding image patch from the contact image and the associated pressure value from the 2D pressure measurements. Image patches were cropped to a fixed size of 64×64 pixels with 3 channel (RGB) and normalized to have a mean (μ) of 0 and a standard deviation (σ) of 1. This standardization facilitated stable and efficient training of the neural network. A supervised learning approach was employed using a convolutional neural network (CNN) for pressure value regression. The network is structured in

four encoder blocks and one fully connected layer with 32 neurons. Each encoder block utilizes a 2D-convolution with a 3x3 kernel, a stride of 2 and a subsequent max-pooling layer. The input to the model is a 64×64×3 image patch, while the output is a single neuron representing the predicted pressure value.

A total of 519,553 parameters are trainable. The model was trained using the Adam optimizer, a regression loss function (MSE), optimizing accurate prediction of pressure values based on the extracted image features. The CNN was trained over a pressure range of 0-14 MPa in eleven load levels, utilizing 400,000 data points for training and 200,000 for validation and testing each. A single data point consists of one 64x64 image patch and its corresponding center pressure value.

Hyperparameter were identified with a parameter sweep over number of convolutional layers and filter depth, number and size of hidden layers and activation functions (LeakyReLU was chosen). A sufficient generalization gap was achieved after 5 epochs which indicates that there still might be too few training samples. The model was tested on unseen spotting images from the pressure area. The training process involved the utilization of spotting images exhibiting medium ink coverage (7.5-8.34 g/m²) on an aluminum sheet with an EDT surface.

This methodology enables a structured and reproducible approach for processing contact images and 2D pressure measurements, facilitating the application of machine learning for predictive modeling in pressure distribution analysis.

## 3 Results and discussion

In a first step the application of spotting paste was investigated assuming a uniform color distribution. It is evident that the distribution of the spotting ink is significantly influenced by the surface structure of the applying ink roller. Upon observation of the entire sheet, the color distribution appears homogeneous. At a magnification of five, a periodic, non-directional pattern can be observed. Intriguingly, the surface structure of the sheet appears to have only a limited effect on the distribution of the ink. Further magnification (20x) reveals areas of increased color density and smaller areas with minimal coloration on the sheet shown with EDT surface (Fig. 2). Similar results can be observed for all other surface topologies.

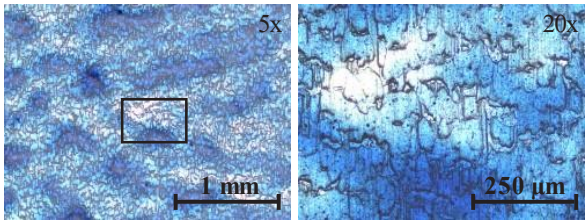


**Fig. 2.** Discernible variations in spotting ink color distribution of a uniformly roller-colored blank with an average layer thickness of 8 µm, 5x and 20x magnified

The distribution of spotting patterns is influenced by the topography of the sheet metal blank's surface under load. However, these patterns are not limited to the surface texture. Fig. 3 shows spotting patterns under different pressures (1 MPa and 7 MPa) for three different surface topologies, which are DC05 (PreTex), EN AW 6016 (EDT) and EN AW 6016 (MF). Each variant is magnified fivefold to observe the detailed patterns. For a more isolated view of the spotting patterns, the contrast was increased by 25%. The key observations are (compare to Fig. 3):

- Higher pressure (7 MPa) leads to a finer and more dispersed spotting pattern compared to lower pressure (1 MPa), where the spotting patterns are more clustered and well-defined.
- All textures exhibit a strong contrast in spotting, with a clear difference between 1 MPa and 7 MPa. The lower pressure results in larger, connected dark spots, while the higher pressure creates more fragmented patterns.
- The DC05 (PreTex) sample displays isolated cluster of ink that are partially interconnected by slight connections.
- EN AW 6016 (EDT) at 1 MPa shows more continuous and interconnected patterns, whereas at 7 MPa, it becomes more fragmented.
- EN AW 6016 (MF) demonstrates enhanced uniform dispersion at both pressures. A comparative analysis shows that 7 MPa exhibits more even distribution compared to 1 MPa, aligning more closely with the sheet metal texture.
- Despite the same material (EN AW 6016), the spotting patterns show differences in an- and isotropic patterns, which can be attributed to MF (anisotropic) and EDT (isotropic) texture.

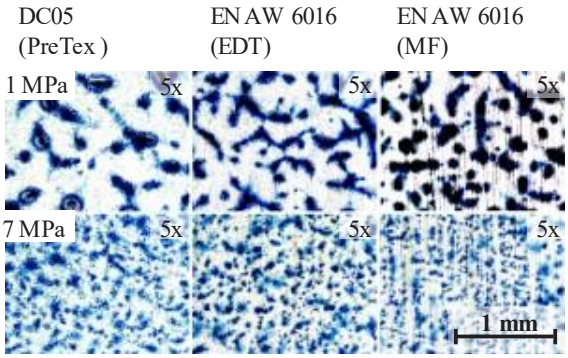


**Fig. 3.** Pressure and surface topology dependencies (PreTex, EDT, MF) of spotting patterns, 5x magnified, contrast enhanced by 25%

Pressure significantly influences the contact behavior and spotting distribution whereas higher pressure reduces the size and increases the dispersion of spots, indicating forced displacement of paste. The surface topology of the sheet metal impacts the pattern formation on lower pressure loads and increasingly loses relevance with increasing the pressure. Isotropy like observed on the isotropic surfaces (PreTex, EDT) leads to clustering of the spotting paste, while anisotropic surfaces (MF) result in a more oriented homogeneous spread.

To describe the color accumulations on the sheet surface depending on the respective topology, the developed interface ratio (Sdr) is used as a reference value. The Sdr value of a completely flat surface is 0. It is defined as:

$$\mathrm{Sdr} = \frac{1}{A}\left(\iint_A \left\{\sqrt{\left[1+\left(\frac{\partial z(x,y)}{\partial x}\right)^2+\left(\frac{\partial z(x,y)}{\partial y}\right)^2\right]}-1\right\}\mathrm{dxdy}\right) \quad (1)$$

The Sdr values of EDT sheet texture demonstrates notable stability when subjected to pressure variations (between 0.096 and 0.107). The developed interface ratio increases progressively with pressure for MF and PreTex sheet metals. The Sdr values of the different surface topologies converge towards the same value which concludes that spotting patterns assimilate at high pressure (Table 2).

**Table 2.** Utilization of the developed interface ratio (Sdr) to compare the ink accumulation based on texture, depending on pressure.

| | **Sdr** | | |
|---|---|---|---|
| load | 1 MPa | 3 MPa | 7 MPa |
| EDT | 0.102 | 0.096 | 0.107 |
| MF | 0.062 | 0.070 | 0.091 |
| PreTex | 0.023 | 0.061 | 0.075 |
| $\Delta Sdr_{min,max}$ | 0.079 | 0.035 | 0.032 |

The tendency of a clustered, more uniform spread at higher pressures based on the Sdr can be observed as shown in Fig. 4. The spotting paste is gradually displaced with higher pressures so that the remaining ink remains along the concave areas of the surface topology.

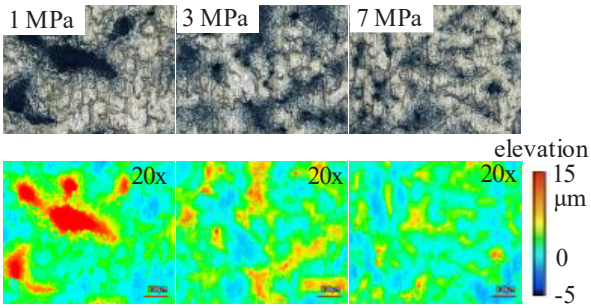


**Fig. 4.** Spotting patterns on EDT textured blank at 1 MPa, 3 MPa and 7 MPa magnified twentyfold (u.), spotting paste distribution as elevation map (l.)

Preloading blanks didn't lead to discernible spotting patterns and showed minor fluctuations in Sdr by less than 10%.

It is anticipated that the results of the microscopic examinations will demonstrate the CNN's sensitivity to alterations in blank texture and ink quantity. Firstly, the pressure prediction for two unseen spotting patterns is presented in Fig. 5.

The measured and predicted pressure values are smoothed by a Gaussian filter in post-processing. This ensures a softer transition of the pressure ranges, which was discretized in the context of CNN processing by segmentation into image sections. The summed pressure forces predicted by CNN were scaled to match the process force.

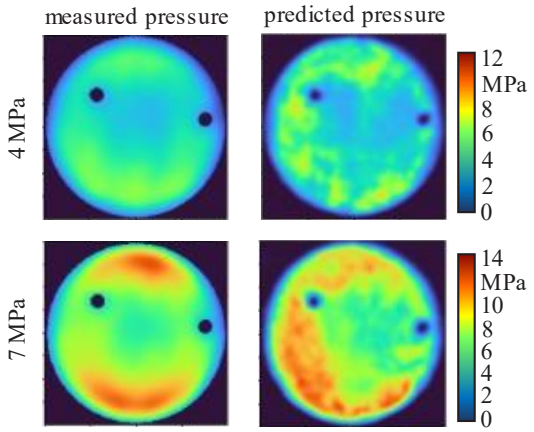


**Fig. 5.** Comparison of measured vs. predicted pressure at different loads

The CNN prediction captures the overall shape and pressure distribution trends but has noticeable differences in intensity and localized variations. The CNN correctly predicts a load increase, as the pressure in the 7 MPa prediction is generally higher than in the 4 MPa prediction. Under higher loads the model tends to overestimate the pressure which can be explained by less training data in the upper pressure ranges. Some fine details in the measured pressure are lost in the prediction, indicating potential limitations in the model's ability to generalize pressure gradients accurately.

Fig. 6 compares ground truth (left column) with CNN-predicted pressure distributions under different applied loads and varying ink quantities. The red box indicates the parameter configuration to which the CNN has been trained. However, it should be noted that all pressure predictions are unseen images of spotting patterns, including those outlined in red.

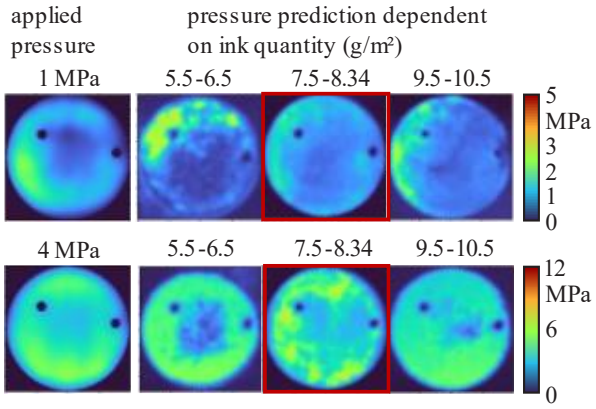


**Fig. 6.** Effect of ink quantity on CNN pressure prediction of unseen data, CNN training configuration is red-bordered

The CNN predictions demonstrate a high degree of similarity to the ground truth images with regard to pressure distribution patterns, though some variations are evident. The pressure distributions shift with changing ink quantities, suggesting the model correctly considers its influence. The CNN predictions demonstrate the greatest accuracy for the 7.5-8.34 g/m² cases (red-bordered images), for which the model was

trained. Conversely, predictions for 5.5-6.5 g/m² and 9.5-10.5 g/m² exhibit minor discrepancies, suggesting a decline in accuracy when extrapolating beyond the conditions that were trained on.

The following results (Fig. 7) put an emphasis on the impact of blank texture on the pressure distribution.

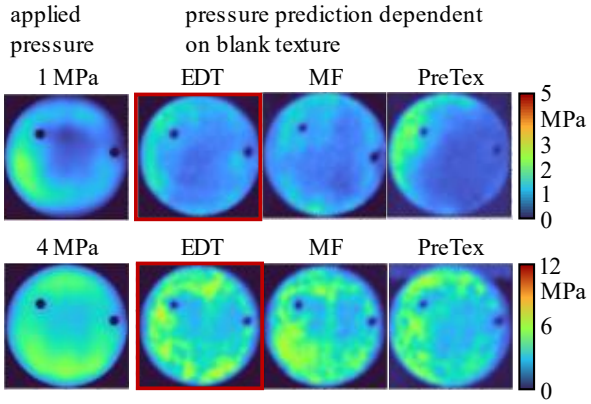


**Fig. 7.** Effect of blank texture on CNN pressure prediction of unseen data, CNN training configuration is red-bordered

The pressure patterns demonstrate variability across different blank textures, thus indicating that texture exerts an influence on the pressure distribution. The precision textured steel blank's results demonstrate a more scattered pressure distribution in comparison to EDT and MF. The conclusions from the previous analysis continue here, in that the predictions for EDT (red-bordered) are most accurate. With regard to the remaining two textures, the model continues to yield satisfactory predictions, notwithstanding minor discrepancies, suggesting a degree of generalisation, in addition to the presence of potential constraints.

Preliminary investigations into understanding the presented CNN indicate that it provides an estimate based on saturation and value/brightness. Furthermore, it has been observed that the CNN also takes into account the substructures/patterns that form within a spotting pattern for the prediction. To this end, the input values for each color channel were scaled by a factor of 0.4-0.8, which did not lead to any major change in the relative pressure distribution up to a certain value (<0.5). A variance of 10% in saturation and a reduction of brightness by 50% showed little to no discernible changes in localized pressure patterns.

## 4 Conclusions

The CNN has successfully learned the overall pressure distribution pattern and its dependency on load, but its accuracy decreases at higher pressures, potentially due to a lack of training data in this range. The overestimation of high-pressure areas above 7 MPa suggests that the model might need additional training data at higher loads to improve its scaling. The localized variations in predicted pressure could be due to noise in the learned representation or insufficient sensitivity to finer details. The results of the microscopic examinations were consistent with the predictions made by the CNN.

It is evident that the CNN has successfully acquired the key features of the spotting patterns, as demonstrated by its capacity to generalise to unseen data. Nevertheless, its accuracy is optimal when predicting within the range of its training reference (red-bordered images). Predictions that deviate from the trained ink quantity range or blank texture result in errors, indicating a necessity for additional training data or enhanced generalisation. The predictions for MF and PreTex blanks are reasonable but show some deviations, likely due to the model having no experience with these textures.

The quantity of colour exerted the most significant influence on the predicted pressure distribution, with the surface texture of the sheets having a secondary impact. The preload condition exhibited minimal fluctuations within the range of 10% across all areas.

Further spotting images and pressure measurements are required to enrich the training data set and implement more complex pressure distributions with larger gradients and jumps. Additionally, the methodology is to be extended from 2D to 3D spotting images to analyse more complex free-form surfaces of car body components across the entire surface. To this end, stitched high-resolution images with a defined projection direction are to be mapped onto scanned components. The validation of the pressure predictions will be achieved through the combination of measurement data and simulated pressure distributions.

## Acknowledgements

This research received funding within the framework of the research project BW1_1435/02 "Fingerprint Press Identification", which was funded by the Invest BW (VwV Invest BW - Innovation II) program of the federal state Baden-Württemberg, Germany. The authors would like to thank the above-mentioned institutions for providing the financial resources, the company FMF-WWF Tool and Prototype Construction GmbH for their technical and material support.

## References

1. A. Birkert, S. Haage and M. Straub *Umformtechnische Herstellung komplexer Karosserieteile. Auslegung von Ziehanlagen*, 427 (2013)
2. P. Essig et al, Conf. Ser.: Mater. Sci. Eng. **651** 012026 (2019)
3. P. Essig et al, Conf. Ser.: Mater. Sci. Eng. **1157** 012025 (2021)
4. A. Zabala, I. Llavori, E. Sáenz de Argandoña, J. Mendiguren, J. of Manuf. Process. **58**, 1285 (2020)
5. F. Göltl et al, Conf. Ser.: Mater. Sci. Eng. **1307** 012039 (2024)
6. M. Hohmann, A. Yiming, L. Penter, S. Ihlenfeldt, O. Niggemann, *An AI Approach for Predicting the Active Surface of Deep Drawing Tools in Try-Out,* at – Automatisierungstechnik, 10.1515/auto-2024-0130 (2024)